THE ROLE OF THE COMPRESSOR ISENTROPIC EFFICIENCY ON NON-INTRUSIVE REFRIGERANT SIDE CHARACTERIZATION OF TRANSCRITICAL CO_2 HEAT PUMP WATER HEATERS

Francisco B. Lamas and Vítor A.F. Costa

Centro de Tecnologia Mecânica e Automação, DEM, Universidade de Aveiro. 3810-193 Aveiro.

Francisco B. Lamas
francisco.lamas@ua.pt

Abstract: *Characterizing the refrigerant side of heat pump water heaters (HPWHs) can be intrusive and expensive. On the other hand, direct external measurement techniques can be unfeasible, particularly in commercial HPWHs for residential applications. Non-intrusive in-situ characterization methods have already been successfully implemented in subcritical heat pumps, providing the refrigerant mass flowrate and the equipment energy performance, by using contact temperature sensors and electric power meters. Subcritical suction and discharge specific enthalpies necessary to apply the method can be obtained from the measured temperatures and their corresponding saturation pressures. Nevertheless, this approach does not apply to the transcritical CO_2 HPWHs. In the supercritical region, temperature and pressure are independent variables, and an iterative process regarding the compressor isentropic efficiency has to be considered. However, when isentropic efficiency data is not available, an additional procedure is required, using a validated gas cooler model to verify the physical reliability of the numerical solutions.*

Keywords: Transcritical CO_2, Heat pump water heater, Compressor isentropic efficiency, Non-intrusive characterization, Gas cooler model

1. INTRODUCTION

Switching heating systems from fossil fuels to low-carbon alternatives is paramount for reaching the European climate objectives for 2030 and carbon neutrality by 2050. Heat pumps assume a primary function to accomplish these targets, using energy from renewable sources (air, water, or geothermal), being (mostly) electrically supplied, energy-efficient, and thus, contributing to a competitive, secure, and low-carbon economy [1]. Nevertheless, energy performance and low-carbon or renewable energy sources are not the only issues dictating their environmental impact. The heat pump technology is predominantly based on vapor- compression refrigeration systems, as in the air-conditioning and refrigeration current technologies. The commonly used refrigerants may substantially contribute to greenhouse gas emissions, particularly the fluorinated-based ones (F-gases) [2]. Atmospheric emissions during the F-gases production, leakages during operation, or even along the recovering, recycling, or destruction processes triggered the relaunch of some natural refrigerants, and among them CO_2. Its environmental harmlessness, safety, low cost, high availability, and unique thermodynamic properties give this ultra-low global warming potential (GWP) operating fluid a significant advantage over other refrigerants [3]. Owing to its low critical temperature (31.1 °C), CO_2 is mainly used in transcritical vapor-compression cycles, and one of the most widespread applications is the transcritical CO_2 heat pump water heater (TCO_2 HPWH) for residential applications, particularly in Japan, where it is known as 'Eco Cute' and rated according to the Japanese energy efficiency standards.

In Europe, the energy performance of electrically driven HPWHs is rated according to the EN16147 standard [4]. However, the energy-performance indicator is used for equipment's comparisons and does not characterize the actual behavior of the HPWHs under a wide range of environmental conditions. On the other hand, it is based on waterside measurements and cannot provide any information for the refrigerant side, commonly obtained with intrusive and expensive equipment [5], unfeasible for *in-situ* measurements [6].

Non-intrusive methodologies applied in air-to-air heat pumps, based on the compressor energy conservation (CEC), demonstrated good accuracy [5,6], besides simplicity, reliability, independence, and non-interference on the system's operation, compared to indoor and outdoor air enthalpy-difference methods [6]. The CEC method allows an accurate estimation of the refrigerant mass flowrate and the equipment energy performance merely using (external) contact temperature sensors and electricity power meters [5,6]. The subcritical suction and discharge specific enthalpies necessary to apply the method are obtained from the measured temperatures and their corresponding saturation pressures. Nevertheless, this method does not apply to the TCO_2 HPWHs. In the supercritical region, where both compressor discharge and gas cooler operating conditions fall, temperature and pressure are variables independent from each other, and an additional parameter or condition has to be considered – in this case, the compressor's isentropic efficiency. One should mention that no *in-situ* nor non-intrusive methods on the refrigerant-side characterization for TCO_2 cycles were found in the literature. This work explores the role of the compressor isentropic efficiency on non-intrusive refrigerant side characterization of TCO_2 HPWHs. The base thermodynamic analysis is presented and includes three versions regarding the compressor isentropic efficiency condition: constant, depending on the pressure ratio through an already known polynomial correlation, or unknown. For the last, an additional methodology is proposed and discussed, based on a validated model for the gas cooler energy balance. It allows obtaining the discharge pressure and determine the compressor isentropic efficiency, thus, enabling non-intrusive HPWHs refrigerant side characterization.

2. METHODOLOGY

Figure 1 exhibits the schematic representation of a TCO_2 HPWH and the respective thermodynamic cycle on the $P-h$ and $T-s$ diagrams. In the TCO_2 HPWH scheme, it is also represented the measurement equipment: 10 non-intrusive (external) contact temperature sensors for both water and refrigerant loops (2 and 8, respectively), one water mass flow meter (easily integrated in the water loop), and one electrical energy/power meter for the entire HPWH. The measurement outputs and variables considered in the following analysis are numbered according to the measurement devices represented in the figure. Note that measurement point 4 is irrelevant for the supercritical gas cooling characterization, yet crucial for an eventual condensation, providing the saturation temperature, similarly to point 8 (or point 7) for the evaporation process.

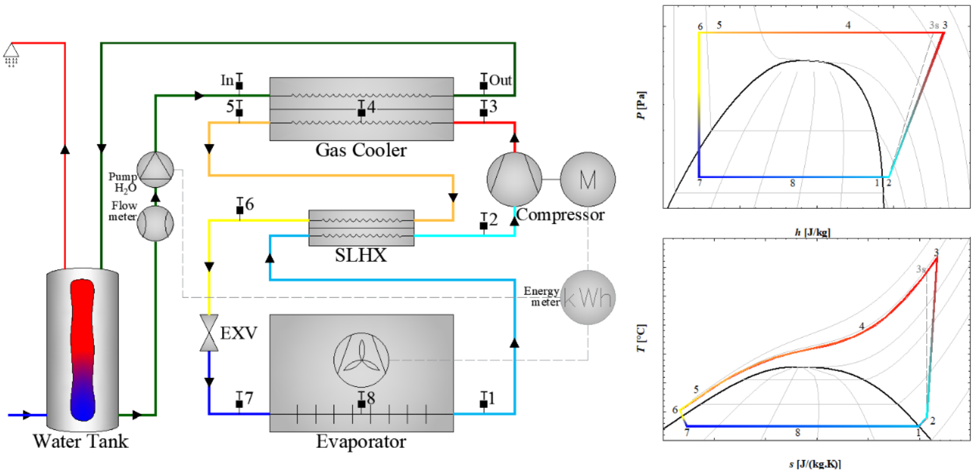

Figure 1. TCO_2 HPWH: scheme (left), and $P - h$ (top left) and $T - s$ (bottom right) diagrams

The coefficient of performance of the whole TCO_2 HPWH is given by the ratio of heat transfer rate in the gas cooler, $\dot{Q}_{gasc}$, to the total electrical input, $\dot{P}_{elec}$,

$$COP = \dot{Q}_{gasc}/\dot{P}_{elec} \tag{1}$$

where the total electrical power input (with the compressor's contribution, $\dot{P}_{elec_{comp}}$, prevailing over the other active components, namely, evaporator fan, water pump and other equipment such as control units, *etc.*) is

$$\dot{P}_{elec} = \dot{P}_{elec_{comp}} + \dot{P}_{elec_{fan}} + \dot{P}_{elec_{pump}} + \dot{P}_{elec_{others}} \tag{2}$$

Neglecting the heat conduction along the tubes' walls and both convective and radiant heat losses to the surroundings (owing to the good thermal insulation commonly used in its external envelope), the energy balance for the gas cooler can be written, for either the water or the refrigerant side, as

$$\begin{cases} \dot{Q}_{gasc} = \dot{m}_{H_2O} \times \bar{c}_{H_2O} \times \Delta T_{H_2O,\,gasc} \\ \dot{Q}_{gasc} = \dot{m}_{CO_2} \times \Delta h_{CO_2,\,gasc} \end{cases} \tag{3}$$

From the previous system of equations, the refrigerant mass flowrate is given by

$$\dot{m}_{CO_2} = \dot{m}_{H_2O} \times \bar{c}_{H_2O} \times \Delta T_{H_2O,\,gasc}/\Delta h_{CO_2,\,gasc} \tag{4}$$

where all the waterside variables can be measured (mass flowrate, $\dot{m}_{H_2O}$, and temperature increase, $\Delta T_{H_2O,\,gasc} = T_{out} - T_{in}$) or calculated (specific heat, $\bar{c}_{H_2O}$). By opposition, the specific enthalpy change on the refrigerant side ($\Delta h_{CO2,\,gasc} = h_3 - h_5$) is unknown and depends on the CO_2 conditions at the gas cooler inlet and outlet, respectively. It becomes clear that the only way to obtain the refrigerant mass flowrate (without measuring it) is by determining both refrigerant specific enthalpies h_3 and h_5.

Using binary functions for the refrigerant properties (non-italic bold), the specific enthalpy results as a function of pressure (P) and temperature (T). Thus, for the gas cooler inlet and outlet, respectively,

$$h_3 = \mathbf{h}(P_3, T_3) \tag{5}$$

$$h_5 = \mathbf{h}(P_5, T_5) \tag{6}$$

Disregarding the pressure drop in the gas cooler, pressure can be considered constant along its length. Therefore, having $P_5 = P_3$ also h_5 becomes dependent on P_3

$$h_5 = \mathbf{h}(P_3, T_5) \tag{7}$$

Finally, the refrigerant mass flowrate, Eq. (4), depends on only one unknown variable, P_3, since both refrigerant temperatures, T_3 and T_5, and the respective specific enthalpies, for that pressure, can be obtained (besides the waterside variables above mentioned)

$$\dot{m}_{CO_2} = \dot{m}_{H_2O} \times \bar{c}_{H_2O} \times (T_{out} - T_{in})/[\mathbf{h}(P_3, T_3) - \mathbf{h}(P_3, T_5)] \tag{8}$$

From the compressor isentropic efficiency definition,

$$\eta_{is} = (h_{3s} - h_2)/(h_3 - h_2) \tag{9}$$

Again, using binary functions for defining h_{3s}, the specific enthalpy at the compressor discharge / gas cooler inlet (point 3s) for the isentropic (ideal) compression and h_2, the specific enthalpy at the compressor suction / SLHX outlet (point 2) similar to Eqs. (5) and (6), and rearranging Eq. (9), it can be presented as

$$\mathbf{h}(P_3, T_3) = \mathbf{h}(P_2, T_2) + [\mathbf{h}(P_{3s}, T_{3s}) - \mathbf{h}(P_2, T_2)]/\eta_{is} \tag{10}$$

Considering the non-pressure drop assumption, in both high and low-pressure sides, and the saturation pressure function (non-italic bold), results in the system of equations

$$\begin{cases} P_{3s} = P_3 \\ P_2 = \mathbf{P_{sat}}(T_8) \end{cases} \tag{11}$$

where T_8 is the evaporation temperature.

The discharge specific entropy and temperature corresponding to the ideal compression can be written as

$$s_{3s} = s_2 = \mathbf{s}(P_2, T_2) \tag{12}$$

$$T_{3s} = \mathbf{T}(P_{3s}, s_{3s}) = \mathbf{T}(P_{3s}, s_2) = \mathbf{T}\big(P_{3s}, \mathbf{s}(P_2, T_2)\big) \tag{13}$$

or, through Eq. (11), respectively, as

$$s_{3s} = \mathbf{s}(\mathbf{P_{sat}}(T_8), T_2) \tag{14}$$

$$T_{3s} = \mathbf{T}\big(P_3, \mathbf{s}(\mathbf{P_{sat}}(T_8), T_2)\big) \tag{15}$$

Applying Eqs. (11), (14), and (15) in Eq. (10),

$$\mathbf{h}(P_3, T_3) = \mathbf{h}(\mathbf{P_{sat}}(T_8), T_2) + \Big[\mathbf{h}\Big(P_3, \mathbf{T}\big(P_3, \mathbf{s}(\mathbf{P_{sat}}(T_8), T_2)\big)\Big) - \mathbf{h}(\mathbf{P_{sat}}(T_8), T_2)\Big]/\eta_{is} \tag{16}$$

At this point, three conditions can be considered regarding the compressor isentropic efficiency, each considered in the following sections.

2.1. Compressor isentropic efficiency known as a constant

Regarding the condition

$$\eta_{is} = C_0 \tag{17}$$

where C_0 is a known and constant value, Eq. (16) can be written as the equality of two generic functions, $\mathbf{f}(x)$ and $\mathbf{g}(x)$, $\forall\, x \in \mathbb{R}^+$, each depending only on P_3, since all other variables, T_2, T_3, and T_8, are known.

$$\mathbf{f}(P_3) = \mathbf{g}(P_3) \tag{18}$$

The equality of the two functions represented in Eq. (18) can be solved through an iterative process, providing P_3. Knowing P_3 value that satisfies, Eq. (16), it is possible to obtain the specific enthalpy at the gas cooler inlet and outlet through Eqs.(5) and (7), respectively. Furthermore, it is possible to determine the refrigerant mass flow rate from the gas cooler energy balance equation written as in Eq. (8).

2.2. Compressor isentropic efficiency given by a polynomial correlation

Many polynomial correlations for the compressor's isentropic efficiency, as functions of the pressure ratio, can be found in the open literature. The most common are fourth-order ($n = 4$) and linear ($n = 1$) correlations [7–9]. However, the polynomial order depends on the compressor type, information provided by the compressor's manufacturer, or on the regression analysis performed by the researchers. Nevertheless, the isentropic efficiency can be represented as

$$\eta_{is} = C_0 + \cdots + C_i \times r^i + \cdots + C_n \times r^n \quad (19)$$

Each C_i with $i \in \{0, 1, \dots, n\}$ is a known and constant empirical value, and r is the pressure ratio, which combined with Eq. (11) results as

$$r = P_3/P_2 = P_3/\mathbf{P_{sat}}(T_8) \quad (20)$$

Once more, also in this case Eq. (16) can be written as the equality of two generic functions, $\mathbf{f}(x)$ and $\mathbf{g}(x)$, each of them depending only on P_3. The process for obtaining P_3 in this case is identical to that when the isentropic efficiency is given by a constant, as described in Section 2.1.

2.3. Unknown compressor isentropic efficiency

Compressor efficiency indicators and performance maps are commonly sensitive proprietary information, therefore, are often inaccessible. For this case, an iterative procedure is needed using a validated numerical model for the gas cooler energy balance. Many dimensional parameters and numerical and/or experimental data are available for that in the open literature. The information varies according to the system purpose (water heating, air conditioning, or refrigeration) and the gas cooler configuration, namely single tube- [10] and multi tubes-in-tube (straight [11] or twisted [12]), microchannel [13], brazed plate [14] or finned-tube [15]. For the TCO_2 HWHP, the most used configuration is the single tube-in-tube gas cooler; and the numerical model is commonly based on the finite volume method, using the logarithmic mean temperature difference approach [3]. The usual outputs of the gas cooler model are the heat transfer rate and the outlet temperatures for the water and CO_2 ($\dot{Q}_{gasc}$, T_{out}, and T_5, respectively); on the other hand, the main inputs are both water mass flowrate and inlet temperature (respectively, $\dot{m}_{H_2O}$ and T_{in}), and the refrigerant mass flowrate and its inlet temperature and pressure ($\dot{m}_{CO_2}$, T_3, and P_3, respectively) [3,10–12,14]. Almost all these variables can be obtained, except P_3 and $\dot{m}_{CO_2}$(which depends on the only unknown variable P_3, as previously seen).

The non-measured input variables of the gas cooler model (P_3 and $\dot{m}_{CO_2}$) are obtained through the process described in Section 2.1, attributing, in each iteration, a value for C_0 in Eq. (17). The process will "sweep" a predefined isentropic efficiency range, providing data sets for the numerical simulation of the gas cooler model. A targeted definition of this range, decreasing the search field, can substantially improve the procedure efficiency by reducing the required computational time. It is proposed, as the lower limit, the compressor isentropic efficiency leading to the minimum pinch-point temperature difference between CO_2 and water temperature profiles, $\eta_{is_{min}}$, as represented on the left-hand side of Figure 2. The higher limit, $\eta_{is_{max}}$, can be defined, at the most, as the unattainable isentropic (ideal) compression, depicted in Figure 2 (right-hand side).

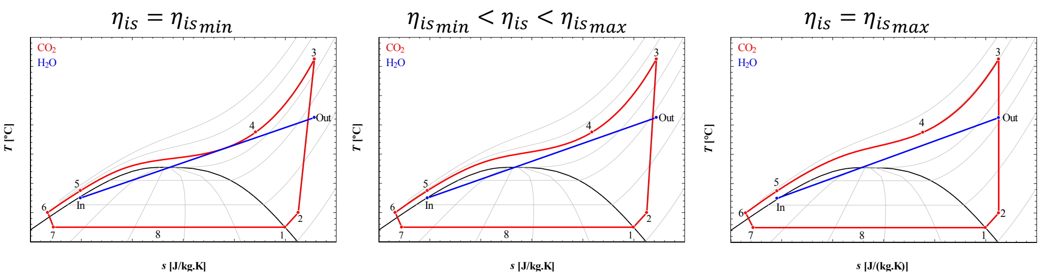

Figure 2. Definition of the search range for η_{is}

However, enlarging the search range increases the computational time. For this reason, $\eta_{is_{max}}$ should be defined as the maximum known technical isentropic efficiency for the specific compressor type under consideration, or, without having this information, it should be considered the maximum technical limit known at the date (around 0.9). The step between successive isentropic efficiencies trials can be adapted, or even refined, according to preliminary, or previous, results from wide-stepped iterations.

Finally, the validated gas cooler model is used to verify the physical reliability of the numerical solutions provided by the first procedure (defined in Section 2.1). As the second iteration process converges (*i.e.*, the isentropic efficiency trial, $\eta_{is_{trial}}$, gets closer to the "real" value, $\eta_{is_{real}}$), the numerical results from the gas cooler model will approximate the experimental ones, as exhibited in Figure 3. The procedure will finish when the three numerical outputs, $\dot{Q}_{gasc}$, T_{out}, and T_5, are simultaneously within the respective and predefined acceptance tolerance. From the results, it is possible to define a correlation for the isentropic efficiency, with the form of Eq. (19), based on the tested pressure ratios.

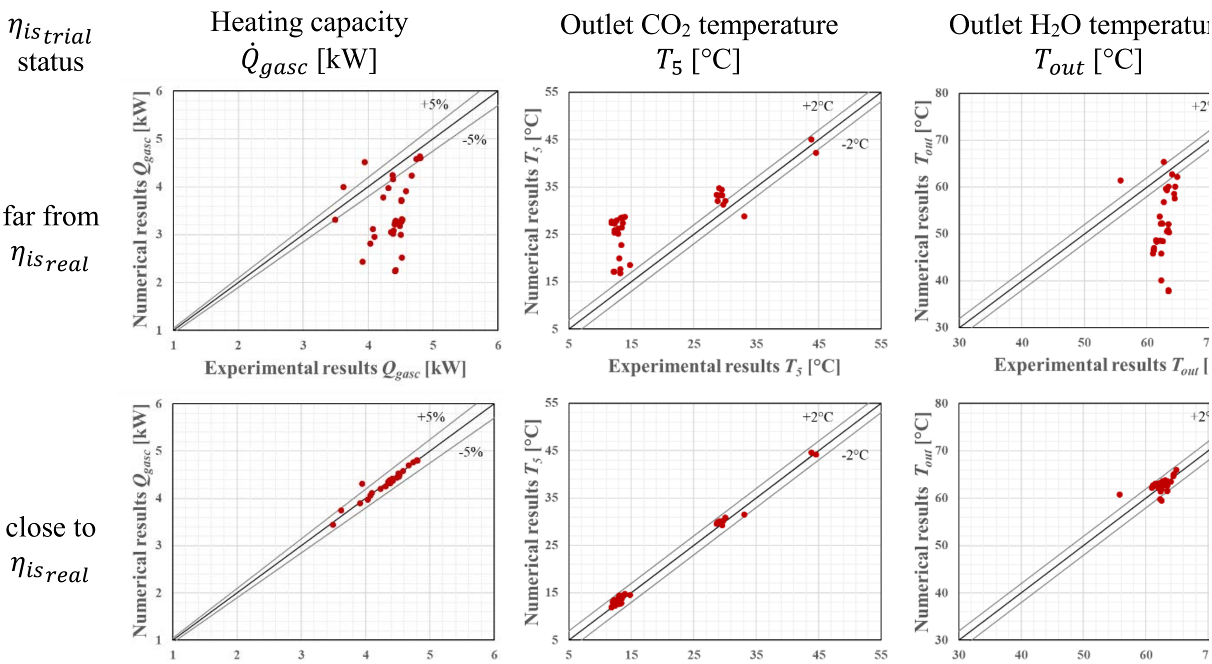

Figure 3. Example of the gas cooler model outputs for different η_{is} trials and working conditions

3. CONCLUSIONS

The thermodynamic basis for a novel non-intrusive refrigerant side characterization of transcritical CO_2 HPWHs is presented, evidencing the role of the compressor isentropic efficiency in the process. The complexity of the proposed methodology depends on the knowledge about the compressor isentropic efficiency. When the compressor data is available, namely its isentropic efficiency, a simple iterative process is sufficient to obtain the discharge pressure since it is the only unknown required to close the equations system. However, when the compressor isentropic efficiency is unknown, another iterative process is required, searching over a range of possible candidates for the compressor isentropic efficiency, and a validated numerical model for the gas cooler energy balance is used to verify the physical reliability of the numerical solutions. The proposed method can be similarly extended to TCO_2 air conditioners and refrigeration systems, regardless of the type of gas cooler, widely contributing and filling the gap in non-intrusive and inexpensive refrigerant side characterization of ultra-low GWP vapor compression systems based on the TCO_2 cycle.

ACKNOWLEDGEMENTS

The present study was developed in the scope of the Smart Green Homes Project [POCI-01-0247-FEDER- 007678], a co-promotion between Bosch Termotecnologia S.A. and the University of Aveiro. It is financed by Portugal 2020 under the Competitiveness and Internationalization OP, and by the European Regional Development Fund (ERDF). This work was funded by the grant SFRH/BD/148378/2019 and the projects UIDB/00481/2020 and UIDP/00481/2020 – FCT-Fundação para a Ciência e Tecnologia; and CENTRO-01- 0145-FEDER-022083 – Centro2020, under the PORTUGAL 2020 Partnership Agreement, through the ERDF.

REFERENCES

[1] European Commission. Directive (EU) 2018/2001 of the European Parliament and of the Council on the promotion of the use of energy from renewable sources. 2018.

[2] European Commission. Regulation (EU) No 517/2014 of the European Parliament and of the Council of 16 April 2014 on fluorinated greenhouse gases and repealing Regulation (EC) No 842/2006. 2014.

[3] Lamas FB, Costa VAF. Finite Volume Model for a Transcritical CO2 Tube-in-Tube Gas Cooler. In: Universidade do Minho, editor. Proc. Congr. Numer. Methods Eng., Guimarães: 2019, p. 350–68.

[4] CEN. EN 16147:2017 Heat pumps with electrically driven compressors - Testing, performance rating and requirements for marking of domestic hot water units. 2017.

[5] Tran CT, Noël D, Rivière P, Arzano C, Marchio D. In-situ method for air-to-air heat pump seasonal performance determination including steady-state and dynamic operations. Int J Refrig 2021;127:239– 49. doi:10.1016/j.ijrefrig.2021.03.001.

[6] Yang Z, Ding L, Xiao H, Zhang G, Wang B, Shi W. All-condition measuring methods for field performance of room air conditioner. Appl Therm Eng 2020;180:115887. doi:10.1016/j.applthermaleng.2020.115887.

[7] Lin KH, Kuo CS, Hsieh W Der, Wang CC. Modeling and simulation of the transcritical CO2 heat pump system. Int J Refrig 2013;36:2048–64. doi:10.1016/j.ijrefrig.2013.08.008.

[8] Minetto S, Cecchinato L, Brignoli R, Marinetti S, Rossetti A. Water-side reversible CO2 heat pump for residential application. Int J Refrig 2016;63:237–50. doi:10.1016/j.ijrefrig.2015.12.015.

[9] Yamaguchi S, Kato D, Saito K, Kawai S. Development and validation of static simulation model for CO2 heat pump. Int J Heat Mass Transf 2011;54:1896–906. doi:10.1016/j.ijheatmasstransfer.2011.01.013.

[10] Song X, Zhang L, Lu D, Shi J, Chen J. Improvement of heat transfer performance and unmatched characteristics of a water-cooled carbon dioxide gas cooler. Appl Therm Eng 2021;197:117326. doi:10.1016/j.applthermaleng.2021.117326.

[11] Sánchez D, Cabello R, Llopis R, Torrella E. Development and validation of a finite element model for water - CO2 coaxial gas-coolers. Appl Energy 2012;93:637–47. doi:10.1016/j.apenergy.2011.12.100.

[12] Yang Y, Li M, Wang K, Ma Y. Study of multi-twisted-tube gas cooler for CO2 heat pump water heaters. Appl Therm Eng 2016;102:204–12. doi:10.1016/j.applthermaleng.2016.03.123.

[13] Huang L, Tao L, Wang C, Yang L. Theoretical and experimental research on using quasi saturation isentropic compression discharge temperature to control refrigerant mass flow rate. Heat Mass Transf Und Stoffuebertragung 2019;55:489–500. doi:10.1007/s00231-018-2437-9.

[14] Zendehboudi A, Ye Z, Hafner A, Andresen T, Skaugen G. Heat transfer and pressure drop of supercritical CO2 in brazed plate heat exchangers of the tri-partite gas cooler. Int J Heat Mass Transf 2021;178:121641. doi:10.1016/j.ijheatmasstransfer.2021.121641.

[15] Marcinichen JB, Thome JR, Pereira RH. Working fluid charge reduction. Part II: Supercritical CO2 gas cooler designed for light commercial appliances. Int J Refrig 2016;65:273–86. doi:10.1016/j.ijrefrig.2015.12.018.